FEBS Letters 584 (2010) 3962–3968

journal homepage: www.FEBSLetters.org

Molecular characterization of β1,4-galactosyltransferase 7 genetic mutations linked to the progeroid form of Ehlers–Danlos syndrome (EDS)

Catherine Bui [a,1,2], Ibtissam Talhaoui [a,1], Matthieu Chabel [a], Guillermo Mulliert [b], Michael W.H. Coughtrie [c], Mohamed Ouzzine [a], Sylvie Fournel-Gigleux [a,*]

[a] UMR 7561 CNRS-Université de Nancy I, Faculté de Médecine, BP 184, 54505 Vandoeuvre-lès-Nancy, France
[b] UMR 7036 CNRS-Université de Nancy I, Faculté des Sciences et Techniques, BP 70329, Vandoeuvre-lès-Nancy, France
[c] Division of Medical Sciences, University of Dundee, Ninewells Hospital & Medical School, Dundee DD1 9SY, United Kingdom

ARTICLE INFO

Article history:
Received 3 June 2010
Revised 26 July 2010
Accepted 2 August 2010
Available online 6 August 2010

Edited by Takashi Gojobori

This work is dedicated to G.J. Dutton who died on the 1st June 2010 and who has been of great inspiration in our study of glucuronosyl- and other glycosyltransferases.

Keywords:
Ehlers–Danlos syndrome
Point mutation
Galactosyltransferase defect
Glycosaminoglycan synthesis
Congenital glycosyltransferase disorder

ABSTRACT

β1,4-Galactosyltransferase 7 (β4GalT7) is a key enzyme initiating glycosaminoglycan (GAG) synthesis. Based on in vitro and ex vivo kinetics studies and structure-based modelling, we molecularly characterized β4GalT7 mutants linked to the progeroid form of Ehlers–Danlos syndrome (EDS), a severe connective tissue disorder. Our results revealed that loss of activity upon L206P substitution due to altered protein folding is the primary cause for the GAG synthesis defect in patients carrying the compound A186D and L206P mutations. We showed that R270C substitution strongly reduced β4GalT7 affinity towards xyloside acceptor, thus affecting GAG chains formation. This study establishes the molecular basis for β4GalT7 defects associated with altered GAG synthesis in EDS.

1. Introduction

Amino acid exchanges in β1,4-galactosyltransferase 7 (β4GalT7, E.C. 2.4.1.133), which is involved in the synthesis of the glycosaminoglycan (GAG) linkage region of proteoglycans, are associated with the pathology of progeroid type Ehlers–Danlos syndrome (EDS) [1]. EDS forms a group of inherited connective tissue disorders characterized by defects in various extracellular matrix proteins including collagens and small leucine-rich proteoglycans, such as decorin. Patients harbouring mutations in the *B4GALT7* gene exhibit aged appearance, developmental delay, dwarfism, craniofacial disproportion and general osteopenia [1,2]. In addition, hypermobile joints, defects in wound healing and loose skin are observed. Aberrant GAG substitution of decorin was initially described in a progeroid EDS patient who carried compound heterozygous amino acid exchanges (A186D/L206P) in β4GalT7 enzyme [3,4]. More recently, two patients exhibiting typical progeroid EDS features including craniofacial appearance, skeletal abnormalities, and aged appearance were described [2]. Sequence analysis of the *B4GALT7* gene from these patients revealed a missense mutation causing the substitution R270C. This defect was found to be associated with reduced galactosyltransferase activity and aberrant GAG substitution of decorin and biglycan in cultured skin fibroblasts [5]. Interestingly, a recent report indicated that in addition to alterations of the dermatan-sulfate chain of decorin, changes in the structure of heparan-sulfate proteoglycans may also contribute to the phenotypic features observed in this β4GalT7-deficient form of EDS, such as altered cell migration and delayed wound repair [6].

Abbreviation: β4GalT7, β1,4-galactosyltransferase 7; EDS, Ehlers–Danlos syndrome; GAG, glycosaminoglycan; Gal, galactose; GlcA, glucuronic acid; 4-MUX, 4-methylumbelliferone-β-D-xylopyranoside; PBS, phosphate buffered saline; Xyl, xylose

* Corresponding author. Address: Sylvie Fournel-Gigleux, UMR 7561 CNRS-Université de Nancy I, Faculté de Médecine, BP 184, 54505 Vandoeuvre-lès-Nancy, France.
E-mail address: sfg@medecine.uhp-nancy.fr (S. Fournel-Gigleux).
[1] These authors equally contributed to this work.
[2] Present address: Institute of Cellular Medicine, Newcastle University, Medical School, Newcastle upon Tyne NE2 4HH, United Kingdom.

0014-5793/$36.00
doi:10.1016/j.febslet.2010.08.001

GAGs are extensively modified linear polysaccharide chains normally attached to core proteins to form proteoglycans. These complex molecules located on the cell surface and in extracellular matrices of virtually every tissue mediate highly diverse key cell events, ranging from mechanical support inside and outside cells to intricate effects on a wide variety of cellular and biochemical processes, such as blood clotting, cell adhesion, differentiation, proliferation and motility [7]. These functions depend on interactions of the GAG chains with a variety of molecules including growth factors, cytokines and their receptors, enzymes such as matrix proteases and coagulation factors, as well as extracellular matrix proteins [8]. The synthesis of GAG chains that govern these functions is initiated by the formation of a tetrasaccharide linkage region composed of glucuronic acid-galactose-galactose-xylose (GlcAβ1,3Galβ1,3Galβ1,4Xyl1-) followed by the elongation of the two main types of GAGs (*i.e.* heparin, heparan-sulfate and chondroitin-/dermatan-sulfate) [9]. The β4GalT7 enzyme catalyses the transfer of a galactose (Gal) residue provided by UDP-α-D-Gal (UDP-Gal) onto Xyl, a key step in the synthesis of the linkage region of GAG chains [10]. Since the formation of this linker tetrasaccharide is required prior to polymerization of both heparan-sulfate and dermatan-/chondroitin-sulfate chains, genetic defects of β4GalT7 strongly affect the biological functions mediated by GAGs, including tissue development and differentiation, leading to severe clinical features that are characteristic of the progeria-type variant forms of EDS [1,2].

Although the alterations in GAG synthesis have been well defined from studies performed in fibroblasts of patients affected by progeroid form of EDS, the consequences of these gene mutations on β4GalT7 properties have not yet been investigated at the molecular level. By site-directed mutagenesis and in vitro and ex vivo kinetic studies, combined to computer-aided modelling of the human protein structure, we deciphered the mechanisms by which the A186D, L206P and R270C mutations affect β4GalT7 function and disrupt GAG synthesis pathways in the EDS congenital glycosylation disorder.

2. Materials and methods

2.1. Materials

4-Methylumbelliferyl-β-D-xylopyranoside (4-MUX), UDP-α-D-galactose (UDP-Gal) were provided by Sigma–Aldrich, and UDP[^{14}C]Gal and $Na_2[S^{35}]SO_4$ was from Perkin–Elmer. The eukaryotic expression vector pcDNA3.1(+) and competent One Shot® Top10 *Escherichia coli* cells were from Invitrogen-Fisher Scientific, and pET-41a(+) vector and *E. coli* BL21(DE3) cells were from Novagen-EMD4Biosciences.

2.2. Expression vector construction

The human β4GalT7 sequence was cloned as previously described [11]. For expression of β4GalT7 in mammalian cells, the full-length cDNA was modified by PCR to include a KpnI site and a Kozak consensus sequence at the 5′ end, and a sequence encoding a myc tag (EQKLIEEDL) and a XbaI site at the 3′ end, prior subcloning into the pcDNA3.1(+) to produce pcDNA-β4GalT7. For bacterial expression, a truncated form of β4GalT7 was expressed as a fusion protein with glutathione-*S*-transferase (GST). The sequence lacking codons for the 60 N-terminal amino acids was amplified from full-length cDNA using the corresponding primers including NcoI and NotI sites and subcloned into the pET-41a(+) vector (Novagen, EMD4Biosciences) to produce plasmid pET-β4GalT7. Mutations were generated using the QuickChange II XL site-directed mutagenesis kit (Stratagene), employing pcDNA-β4GalT7 or pET-β4GalT7 plasmids as template, and sense and antisense primers listed in Table 1 (Supplementary data).

Table 1
Kinetic parameters of wild-type β4GalT7 and R270C EDS mutant for donor UDP-Gal and the acceptor 4-MUX.

Enzyme	K_A (mM) UDP-Gal	K_B (mM) 4-MUX	K_{ia} (mM)	k_{cat} (s^{-1})
β4GalT7	0.45 ± 0.09	0.61 ± 0.08	0.09 ± 0.03	1.14
R270C	0.46 ± 0.16	6.12 ± 0.96	0.29 ± 0.09	ND

Kinetic parameters towards donor and acceptor substrates were evaluated by double substrate kinetics using 0.2 μg purified GST-β4GalT7 protein at concentrations of UDP-Gal and of 4-MUX varying from 0 to 5 mM. Data were fitted to Eq. (1) described in Section 2 by non-linear least square regression analysis using the curve-fitter program of SigmaPlot 9.0. ND, not determined, *i.e.* no k_{cat} could not be accurately evaluated for R270C mutant since 4-MUX is poorly soluble at concentration higher than 10 mM required to achieve acceptor substrate saturation.

2.3. Heterologous expression of wild-type and mutated β4GalT7

CHO pgsB-618 cells defective in β4GalT7 activity established by Esko et al. [12] were purchased from the American Type Culture Collection (ATCC). Cultured cells were individually transfected at 80% confluency with wild-type and mutated pcDNA-β4GalT7 plasmids using ExGen 500 reagent (Euromedex, Souffelweyersheim, France), according to the manufacturer's recommendations. Cells were harvested in phosphate buffered saline (PBS) 48 h after transfection, pelleted by centrifugation at 5000×*g*, resuspended in 0.25 M sucrose, 5 mM HEPES buffer (pH 7.4) and sonicated three-fold 5 s. Protein concentration was determined by the method of Bradford [13] prior to SDS–PAGE or activity analyses. Alternatively, transfected cells were transferred to labelling medium in the presence of 4-MUX prior to GAG isolation, as described below.

To express wild-type and mutated GST-β4GalT7, *E. coli* BL21(DE3) cells harbouring pET-β4GalT7 expression vector were grown in Luria-Bertani (LB) medium and gene expression was induced with 1 mM isopropyl-β-D-thiogalactopyranoside (IPTG, Sigma–Aldrich) added to bacteria cultured at 20 °C for 16 h. GST-β4GalT7 proteins were purified by affinity chromatography using Glutathione Sepharose™ 4B columns (GE Healthcare Life Sciences).

2.4. Galactosyltransferase activity

The in vitro assay of β4GalT7 activity was performed as previously described [11]. Reactions were performed in 100 mM sodium cacodylate buffer (pH 7.4) containing 10 mM $MnCl_2$, 1 mM UDP-Gal, 0.05 μCi UDP[U^{14}C]Gal, 5 mM 4-MUX and 40 μg of total cell protein or 0.2 μg purified protein. Incubations were carried out at 37 °C for 30–60 min in a total volume of 50 μl, and reaction products were separated by thin layer chromatography [14,15]. For kinetic studies, reaction products were analyzed by high performance liquid chromatography (HPLC) using a reverse phase C_{18} column attached to a Waters e2695 instrument equipped with a Berthold FLowStar radioactivity monitor.

2.5. Kinetic analyses

The kinetic parameters for UDP-Gal and 4-MUX were determined using double substrate kinetics with concentrations of UDP-Gal and 4-MUX varying between 0 and 5 mM by non-linear regression using Sigma Plot™. Data were analyzed for a two-substrate system by fitting to an equation for sequential symmetrical initial velocity pattern, equation below (ordered or random equilibrium mechanism) [16,17]. In this equation V_{max} is the maximum velocity, [A] is the concentration of UDP-Gal, and [B] the concentration of 4-MUX. K_a and K_b are the true K_m for donor and acceptor substrates and K_{ia} is the dissociation constant for UDP-Gal.

$$v = \frac{V_{max}[A][B]}{K_{ia}K_B + K_B[A] + K_A[B] + [A][B]} \quad (1)$$

2.6. Analysis of GAG synthesis by $Na_2[^{35}S]SO_4$ incorporation

To analyze GAG chain synthesis initiated from exogenously added xyloside, CHO pgsB-618 cells transfected with wild-type, mutant pcDNA-β4GalT7, or empty vector (mock) were incubated for 12 h in Fischer's medium containing 10 μCi/ml $Na_2[^{35}S]SO_4$ in the presence or absence of 4-MUX (0–10 μM). Medium (1 ml) was applied to a G-50 column to separate non-incorporated radiolabelled sulfate, and GAGs present in the eluates were quantified by scintillation counting or resolved by SDS–PAGE using Criterion Precast gels (4–15% Bis–Tris, Bio-Rad) and visualized by autoradiography.

2.7. Indirect immunofluorescence staining of recombinant CHO pgsB-618 cells

Indirect immunofluorescence staining of cell surface proteoglycan GAG chains in CHO pgsB-618 transfected cells was performed as previously described [18], using mouse anti-heparan-sulfate primary antibodies (10E4 [19], Seikagaku Corporation) and AlexaFluor 488-conjugated goat anti-mouse secondary antibodies (Molecular Probes/Invitrogen). Wild-type and mutated β4GalT7 proteins expressed in CHO pgsB-618 transfected cells were simultanously immunostained following Triton-X100-permeabilization using anti-myc primary antibodies and AlexaFluor 594-conjugated goat anti-mouse secondary antibodies, following the same procedure.

2.8. Molecular modelling of human β4GalT7 structure

The molecular model of the human β4GalT7 was built using Modeller version 8v2 [20], based of the structure of monomer A of bovine β4GalT1 complexed with UDP-Gal (PDB entry 1O0R) [21]. The energy of the resulting model was minimized using the Amber simulation program version 8 [22]. Charges of the atoms of UDP-Gal were calculated using the GAUSSIAN94 package [23] and the HF/6-31 G* basis set. Atom-centered charges were fitted with Antechamber module of Amber 8 [22]. Mn^{2+} parameters available from Amber site (http://ambermd.org). Docking of UDP-Gal–Mn^{2+} complex in the human β4GalT7 structure was performed manually based on the position of this ligand in bovine β4GalT1. The whole system was solvated, the energy was minimized and submitted to molecular dynamics at 300 K. A model for a *O*-β-D-xylosylpeptide corresponding to the 15 N-terminal amino acids of human decorin (EDEA**S**GIGPEVPDDR) containing Xyl attached to Ser Oγ (*N*-decorin-Xyl) was generated using the AMBER/GLYCAM Input Configurator server (http://glycam.ccrc.uga.edu/AMBER). Docking *N*-decorin-Xyl into β4GalT7 acceptor binding site was performed manually based on the position of the first *N*-acetyl-D-glucosamine in the structure of bovine β4GalT1 (PDB entry 1TW5), and this model was submitted to energy minimization and molecular dynamics as described above. Finally, the model of human β4GalT7 was compared to the crystal structure of Drosophila β4GalT7 (PDB entry 3LW6) using the Dali program for protein structure comparison available at http://ekhidna.biocenter.helsinki.fi/daliserver/ [24].

2.9. Statistical analyses

All data are presented as mean ± S.D. of three determinations on at least two sets of experiments. For comparison among multiple groups, one-way analysis of variance (ANOVA) followed by Bonferroni post-hoc correction test was used. Statistical analyses were performed using GraphPad Prism software (version 5.0).

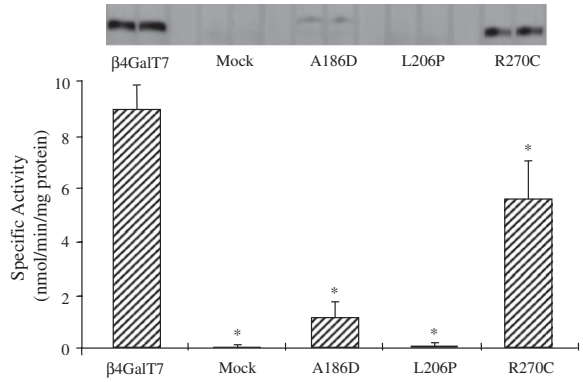

Fig. 1. Galactosyltransferase activity of EDS-β4GalT7 mutants expressed in CHO pgsB-618 towards 4-MUX. Activity of wild-type and mutant enzymes was evaluated using 5 mM 4-MUX and 1 mM UDP-Gal (0.05 μCi UDP[$U^{14}C$]Gal) in the presence of 40 μg cell homogenate. The reaction products were separated by thin layer chromatography, visualized by autoradiography (shown in inset) and quantified by scintillation counting. Data are the mean ± S.D. $n = 3$, $^{*}P < 0.05$.

3. Results

3.1. EDS mutants exhibit large differences in β4GalT7 activity and kinetic properties

Wild-type β4GalT7, and A186D, L206P and R270C mutants were expressed as full-length proteins in CHO pgsB-618 cells and tested for in vitro galactosyltransferase activity using 4-MUX as acceptor substrate. Fig. 1 revealed large differences in galactosyltransferase activity between wild-type and mutant enzymes, although the recombinant proteins were expressed at similar level, as indicated by immunoblot analysis using anti-myc antibodies (not shown). The β4GalT7-A186D mutant exhibited nine-times lower activity than wild-type, whereas substitution of Leu206 with Pro led to an inactive enzyme. The β4GalT7-R270C mutant catalyzed the transfer of Gal onto 4-MUX with a specific activity reaching about 60% that of the wild-type enzyme.

To further analyze the kinetic properties of EDS-β4GalT7 mutants, the catalytic domain of wild-type and mutant enzymes was produced as a soluble protein fused to GST in *E. coli*. The recombinant wild-type enzyme, and β4GalT7-A186D and R270C mutants were purified to apparent homogeneity by affinity chromatography (Fig. 2). Determination of the kinetic parameters of the purified enzymes showed that the wild-type GST- β4GalT7 fusion protein was highly active with a k_{cat} up to 1.1 s^{-1} (Table 1). Furthermore, the K_m value of this enzyme towards UDP-Gal and 4-MUX was about 0.45 mM and 0.60 mM, respectively. These values are in the same range as apparent K_m determined for the membrane-bound enzyme expressed in HeLa cells (data not shown), indicating that expression of the catalytic domain, *i.e.* lacking the transmembrane domain and stem region did not substantially affect substrate binding and catalytic properties of the enzyme. The K_m value for GST-β4GalT7 towards UDP-Gal was also in the same range as reported by Pasek et al. [25], for the human β4GalT7 expressed in fusion with galectin (*i.e.* 0.51 mM).

Consistent with the low level of activity detected for the β4GalT7-A186D mutant expressed in deficient CHO cells, this variant showed little activity when produced in bacteria, preventing further kinetic analyses. The β4GalT7-L206P mutant, which lacked activity in eukaryotic cells, was mainly produced as insoluble inactive protein when expressed in *E. coli* (Fig. 2). These results indicate that exchange of leucine at position 206 to a proline

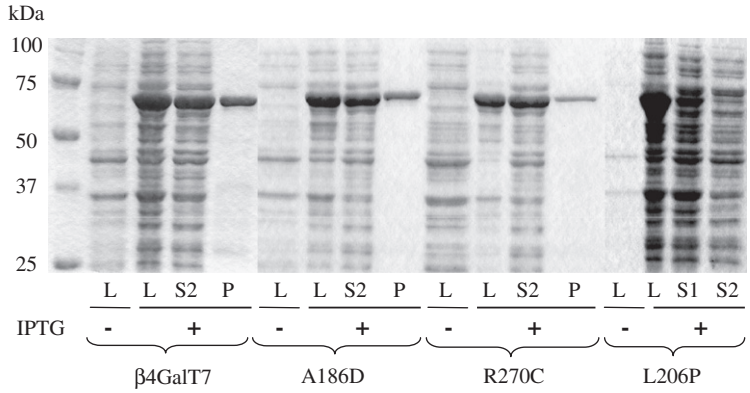

Fig. 2. Expression and purification of EDS-β4GalT7 mutants in *E. coli*. Wild-type GalT7 and mutated proteins were expressed in *E. coli*, and A186D, and R270C mutants were purified from supernatant of 12 000×*g* centrifugation by affinity chromatography. Proteins were analyzed by SDS–PAGE and stained with Coomassie Brilliant Blue. Shown from left to right, cell lysate from uninduced and IPTG-induced bacteria (L, 25 μg), 12 000×*g* supernatant (S2, 12 μg) and purified fusion protein (P, 1–3 μg). S1 refers to 5000×*g* supernatant from cell lysates expressing β4GalT7-L206P mutant.

residue probably affected protein folding and dramatically impaired its function. In contrast, substitution of Arg270 to cysteine resulted in a β4GalT7 protein which retained activity. Interestingly, whereas the K_m value of the β4GalT7-R270C mutant towards UDP-Gal was similar to that of the wild-type enzyme, its affinity for the xyloside acceptor substrate 4-MUX was dramatically reduced (10-times higher K_m value compared to wild-type).

3.2. Molecular modelling of human β4GalT7

A molecular model of human β4GalT7 was built based on the structure of bovine β4GalT1 in complex with UDP-Gal molecule (PDB 1O0R). The position of A186, L206 and R270 are highlighted in the structure is shown in Fig. 5, panel A. We also used the crystal structure of the bovine β4GalT1 in complex with an oligosaccharide acceptor substrate, as template (PDB 1TW5), to generate a model of the human β4GalT7 acceptor binding site containing *N*-decorin-Xyl. The results shown Fig. 5B suggest a potential interaction between Arg270 and the serine residue of decorin peptide. Furthermore, we carried out a superimposition of the modelled human β4GalT7 and of the crystal structure of Drosophila β4GalT7 (PDB 3LW6 [26]), by structure alignment using Dali program [24] (Supplementary data, Fig. 1). The results show a Z-score of 22.8 and a RMSD (Root mean standard deviation) of 2.6 Å, indicating a good fit between the structures of modelled human and Drosophila β4GalT7. The two structures exhibit a very similar organization of the core protein with Ala186 and Leu206 (numbered in human β4GalT7) located in a secondary structure environment similar to that of Ala169 and Val189 (numbered in fly β4GalT7) (Supplementary data, Fig. 1). On the other hand, Arg270 is located at the surface of the protein, in a less conserved structural domain between human and fly β4GalT7 proteins. In the case of the protein from Drosophila, this domain contains a disulfide bond between Cys255 and Cys310 [26], which is not present in human, contributing to a different secondary structure of the C-terminal part of the β4GalT7 protein compared to its human counterpart domain containing Arg270.

3.3. Effect of EDS mutations on GAG synthesis in CHO pgsB-618 cells

We next designed a series of experiments to determine the functional consequences of EDS mutations on β4GalT7 activity ex vivo. For this purpose, we analyzed the capacity of wild-type and mutated enzymes to prime GAG synthesis on the exogenous β-D-xyloside 4-MUX, in β4GalT7-deficient CHO pgsB-618 cells. The rate of GAG synthesis was evaluated in recombinant cells as a function of xyloside concentration. Results shown in Fig. 3A indicate that expression of wild-type β4GalT7 in these cells induced a concentration-dependent increase in GAG synthesis. No detectable [$^{35}SO_4$]-incorporation was detected in mock-transfected cells, up to 10 μM 4-MUX concentration (Fig. 3A). In confirmation of these observations, SDS–PAGE analysis revealed the presence of radiolabelled GAG chains in β4GalT7-transfected CHO psgB-618 cells upon addition of 4-MUX, whereas no radioactivity could be detected in mock-transfected cells, or when addition of xyloside was omitted (Fig. 3B). Interestingly, although the β4GalT7-A186D mutant exhibited low in vitro enzyme activity, this variant was able to prime GAG synthesis in CHO deficient cells up to a synthesis rate reaching two-third that of the wild-type enzyme at the highest concentration of 4-MUX (Fig. 3A). The presence of radiolabelled

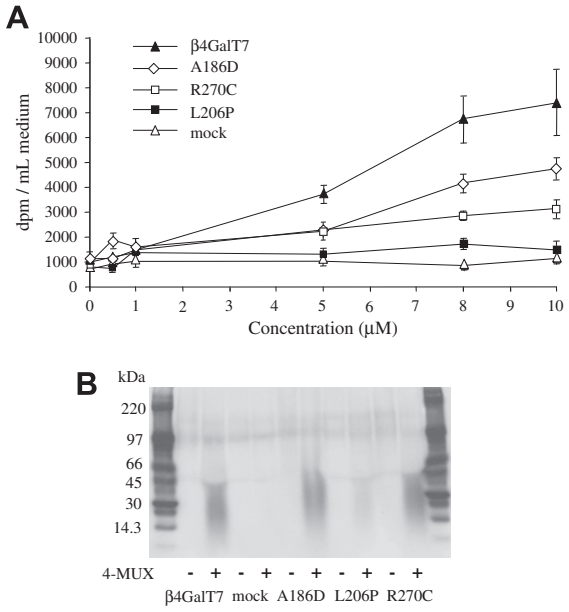

Fig. 3. Kinetics of GAG chain synthesis from 4-MUX in CHO pgsB-618 cells expressing wild-type or EDS-β4GalT7 mutants. Cells seeded at 6×10^5 cells in six-well plates were individually transfected with pcDNA-β4GalT7 or A186D, L206P, and R270C mutants. (A) Kinetics of GAG synthesis as a function of 4-MUX-concentration. 24H following transfection, cells were incubated in the presence of $Na_2[^{35}SO_4]$ and increasing concentrations of 4-MUX for 12 h before GAG isolation and quantification by scintillation counting. (B) Gel electrophoresis of radiolabelled GAG chains isolated from conditioned medium of recombinant CHO pgsB-618 cells incubated in the presence of $Na_2[^{35}SO_4]$ and 4-MUX (5 μM).

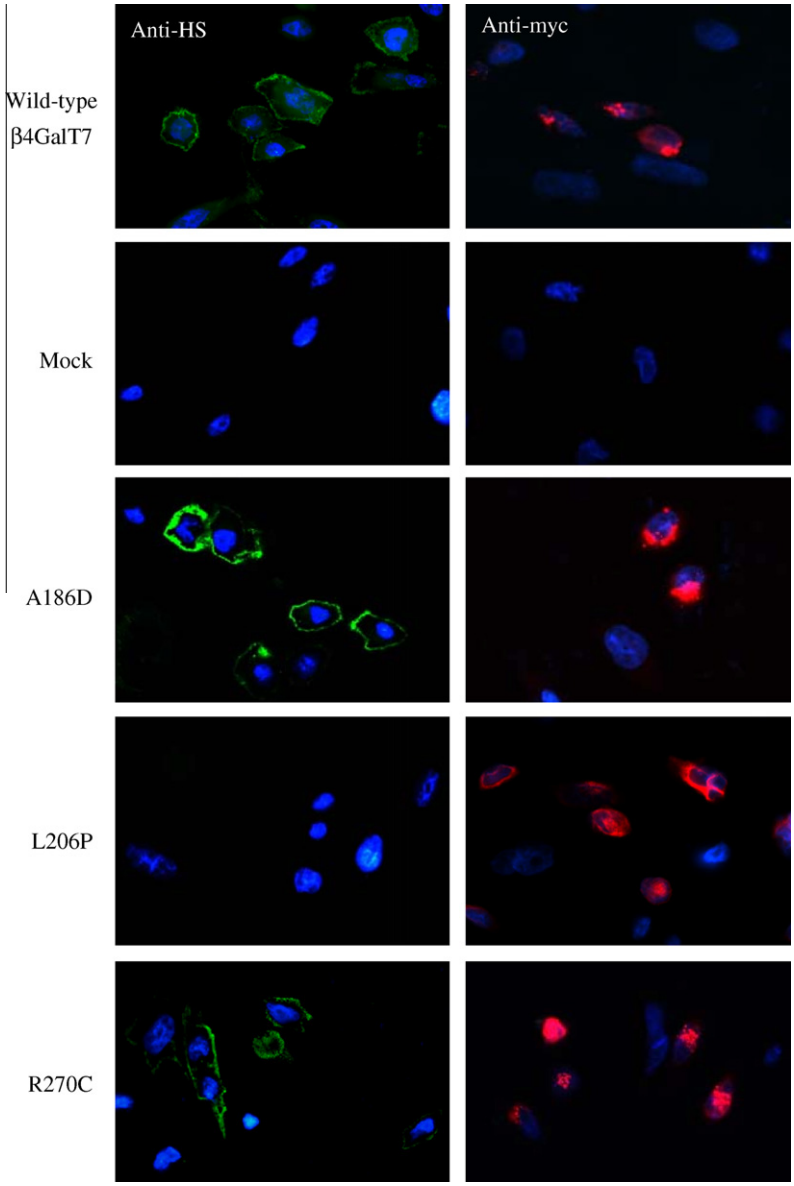

Fig. 4. Heparan-sulfate expression in CHO pgsB-618 cells transfected with EDS-β4GalT7 mutants. Cells were transfected with pcDNA-β4GalT7, A186D, L206P, or R270C or mock-transfected and indirect immunofluorescence staining was performed using 10E4 anti-heparan-sulfate (anti-HS, left panels), or following permeabilisation using anti-myc antibodies (right panels). Nuclei were stained by Hoechst reagent prior to mounting slides.

GAG chains was confirmed by SDS–PAGE analysis in the culture medium of cells transfected by this mutant in the presence of 4-MUX (Fig. 3B). Furthermore, the β4GalT7-L206P mutant exhibited no GAG priming activity towards 4-MUX in transfected cells, consistent with the lack of galactosyltransferase activity observed for this enzyme in vitro. In agreement, no radiolabelled GAG chains were observed upon gel electrophoresis analysis in those cells, in the presence of 4-MUX (Fig. 3). β4GalT7-R270C mutant was able to produce a significant increase in GAG synthesis rate as a function of 4-MUX concentration, although at a lower level compared to the wild-type enzyme. This result is in agreement with the in vitro kinetic properties of this mutant, which were characterized by a strong decrease in affinity towards xyloside acceptor substrate and reduced efficiency compared to the wild-type β4GalT7.

To further determine the consequences of EDS mutations on GAG synthesis, we carried out immunofluorescence analyses of heparan-sulfate expression in β4GalT7-defective CHO pgsB-618 cells transfected with the corresponding cDNAs, since it was previously reported that wild-type CHO-K1 cells predominantly produce heparan-sulfate GAG chains [12]. A prominent staining of cell membrane heparan-sulfates by 10E4 antibodies (anti-heparan-sulfate), was observed in CHO-pgsB-618 cells transfected with wild-type β4GalT7, and this staining pattern was associated with typical Golgi pattern of the recombinant protein revealed with anti-myc antibodies (Fig. 4). As expected, no heparan-sulfate expression could be detected in mock-transfected CHO pgsB-618 cells by indirect immunofluorescence analysis. The intracellular location of β4GalT7-A186D, and of β4GalT7-R270C mutant was similar to that of the wild-type exhibiting typical Golgi staining (Fig. 4). In addition, these mutants were able to restore heparan-sulfate cell surface expression revealed by 10E4 antibodies, confirming ex vivo galactosyltransferase analyses indicating that they were able to sustain, at least partially, GAG chain priming in deficient CHO cells. By contrast, although the β4GalT7-L206P mutant was expressed, as shown by intracellular staining using anti-myc antibodies, no membrane staining of cellular heparan-sulfate could

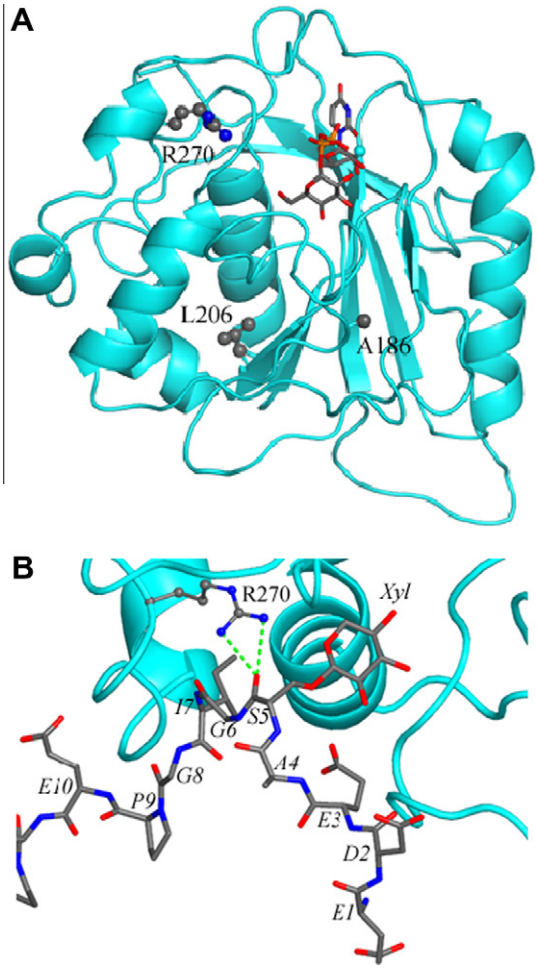

Fig. 5. Molecular modelling of human β4GalT7 structure. (A) The model of β4GalT7 based on bovine β4GalT1 in complex with UDP-Gal (PDB entry 1O0R) is shown in "ribbon" and of UDP-Gal in "sticks". Positions of Ala186, Leu206 and Arg270 are highlighted in "balls-and-sticks". (B) The model of the acceptor binding site of human β4GalT7. Protein *N*-decorin-Xyl in "sticks". Hydrogen bonds between Arg270 (β4GalT7) and the main chain of Ser5 attached to Xyl (*N*-decorin-Xyl) are shown in green dotted lines.

be seen, confirming that this mutant exerted the most severe effect on GAG synthesis. Similar to previous report [4], expression of this mutant exhibited a diffuse pattern (Fig. 4), suggesting altogether that L206P substitution results in a conformational change of the β4GalT7 protein, loss of activity and altered intracellular trafficking.

4. Discussion

Individuals affected by the progeroid-type EDS suffer from severe clinical manifestations including craniofacial and skeletal abnormalities, developmental retardation and aged appearance [1]. Although detailed studies on the mechanisms of GAG alterations contributing to the complex pathology of this genetic disorder have been carried out in skin fibroblasts from affected patients [5,6], the molecular basis underlying β4GalT7 deficiency is not yet fully understood. Here, we investigated the molecular consequences of progeroid-type EDS mutations A186D, L206P, and R270C on (i) β4GalT7 enzyme activity and kinetic properties in vitro, and (ii) ex vivo GAG chain synthesis in defective CHO pgsB-618 cells. These approaches, combined with computer-aided modelling of the structure of human β4GalT7 and its acceptor binding site, allowed us to elucidate the mechanisms underlying β4GalT7 functional defects in EDS congenital glycosylation disorder. The β4GalT7-deficient CHO pgsB-618 line was transfected with wild-type, A186D, L206P or R270C cDNA with the resulting pattern of activities, (i) β4GalT7-A186D mutant exhibited about 10% activity of wild-type; (ii) mutation of leucine at position 206 to proline abolished activity; (iii) galactosyltransferase activity of the β4GalT7-R270C mutant was reduced two-fold compared to wild-type. To assess the functional consequences of the mutations in CHO pgsB-618 transfected cells, we developed two approaches. Firstly, we studied the effect of the supplementation of 4-MUX on GAG synthesis. Secondly, we analyzed the restoration of heparan-sulfate expression by indirect immunofluorescence analysis. Ex vivo kinetic studies of GAG synthesis revealed that expression of the β4GalT7-A186D mutant partially restored GAG priming compared to the wild-type enzyme. Immunostaining of heparan-sulfate chains in β4GalT7-A186D transfected cells also revealed a pattern similar to that observed upon expression of the wild-type enzyme. These observations corroborate previous report indicating that this mutant restored GAG synthesis based on flow cytometry analysis [4]. It should be noted that the reduction in β4GalT7 galactosyltransferase activity in vitro due to the A186D substitution was greater than the decrease in GAG priming evaluated in the CHO pgsB-618. Interestingly, it was reported that this mutation caused a larger reduction in apparent K_m of β4GalT7 towards UDP-Gal than acceptor substrate [10]. Since UDP-Gal serves as a sugar donor for several galactosyltransferases involved in glycoprotein and GAG synthesis, the concentration of this molecule might not been rate-limiting, thus possibly explaining the moderate effect of the β4GalT7-A186D mutation ex vivo.

Comparison of the consequences of the three genetic mutations of β4GalT7 causing the progeroid form of EDS revealed that only substitution of leucine at position 206 with proline, led to a complete loss of enzyme activity. Our results showed that this mutant was unable to prime GAG synthesis from exogenous xyloside 4-MUX, nor restore heparan-sulfate expression in CHO pgsB-618 defective cells. Molecular modelling of the human β4GalT7 protein, comparison of this model to the crystal structure of the Drosophila β4GalT7 [26], and multiple sequence alignment studies provide clues to explain this effect. Indeed, Leu206 is strongly conserved in β4GalT7-related sequences among various animal species (Talhaoui, I., Oriol, R. et al. unpublished). In our model of the human β4GalT7 structure (see Fig. 5A), this residue is positioned in a small conserved β-sheet, similarly to its counterpart Val189 in Drosophila β4GalT7 3D structure (see Fig. 1 Supplementary data). Introduction of a proline residue at this position has been predicted to disrupt the secondary or even the tertiary structure of the protein [26]. In agreement with this assumption, we found that in contrast to other EDS mutants, the catalytic domain of β4GalT7-L206P was expressed as insoluble inactive material in *E. coli*.

It was previously shown by Seidler et al. [5] that β4GalT7 activity towards *para*-nitrophenyl-Xyl in skin fibroblasts of patient harbouring the R270D mutation was reduced compared to fibroblasts from healthy patients. In agreement with this finding, comparison of in vitro and ex vivo activity of β4GalT7-R270C mutant expressed in CHO pgsB-618-defective cells showed a decrease of both in vitro galactosyltransferase activity and GAG priming. Investigation of the kinetic properties of the purified mutant enzyme following expression in *E. coli* shed light on the biochemical basis of β4GalT7-altered function upon mutation. A large decrease in affinity towards 4-MUX acceptor substrate was noticed for this mutant, suggesting that arginine to cysteine replacement at position 270 may alter the organization of the acceptor binding site. An increase in K_m value upon R270C mutation was also observed when using a synthetic glycine-serine-Xyl derivative as acceptor substrate (data not shown). Interestingly, molecular modelling of β4GalT7 bound to Xyl attached to the serine of a decorin peptide predicted that

Arg270 is located in the vicinity of the core protein of this proteoglycan (Fig. 5B), which glycanation is affected in EDS [5]. In the Drosophila structure, it has been found that Lys254 (corresponding to Arg270 in primary sequence alignment) is located at the C-terminal end of the long flexible loop (residues 242–255), and the authors predicted that a cysteine substitution may affect the conformational flexibility of this loop [26]. Noteworthy, protein comparison of the C-terminal domain containing Arg270 indicates that human and Drosophila β4GalT7 structures present a different secondary structure organization. Therefore, crystal structure resolution of the human β4GalT7 in complex with acceptor substrate is required to definitively establish the consequences of R270C-EDS mutation.

In conclusion, based on current results, we propose the following molecular basis underlying progeroid type EDS. (1) Although the Ala186 to aspartate replacement strongly reduced in vitro β4GalT7 enzyme activity when expressed in deficient-CHO pgsB-618 cells and in *E. coli*, the consequences of this mutation on GAG synthesis are much less pronounced. This finding suggests that this mutation is not the primary cause for the alteration of GAG synthesis observed in the EDS patient carrying the compound A186D and L206P mutations. (2) In contrast, the dramatic effect of L206P both on in vitro and ex vivo β4GalT7 activity can be attributed to a major conformational change induced by the leucine to proline substitution at this position. This is likely to account for the alteration of GAG synthesis in the progeroid EDS patient carrying the compound mutations. (3) The β4GalT7-R270C mutant exhibited a strong decrease in affinity together with a decreased catalytic efficiency that translated into a reduced ability to prime GAG synthesis upon expression in β4GalT7-deficient cells. These molecular alterations are likely to cause the altered GAG structure and connective tissue disorder observed in the patient carrying a homozygous mutation of β4GalT7 at this position.

Acknowlegdments

Dr. J.-C. Jacquinet (UMR CNRS 6005, University of Orléans, France) is gratefully acknowledged for providing glycine-serine-Xyl. This work was supported by The Agence Nationale de la Recherche (GAGNetwork ANR-08-PCVI-0023-01), CI2 INSERM-University of Dundee, Royal Society International Joined Program, Région Lorraine, Communauté Urbaine du Grand Nancy, CNRS and University Henri Poincaré Nancy I. Part of this work was performed under the auspices of an EAL (European Associated Laboratory) between UMR CNRS 7561-UHP Nancy 1 and the University of Dundee. Ibtissam Talhaoui is recipient of a MRST PhD fellowship.

Appendix A. Supplementary data

Supplementary data associated with this article can be found, in the online version, at doi:10.1016/j.febslet.2010.08.001.

References

[1] Kresse, H., Rosthoj, S., Quentin, E., Hollmann, J., Glossl, J., Okada, S. and Tonnesen, T. (1987) Glycosaminoglycan-free small proteoglycan core protein is secreted by fibroblasts from a patient with a syndrome resembling progeroid. Am. J. Hum. Genet. 41, 436–453.
[2] Faiyaz-Ul-Haque, M., Zaidi, S.H., Al-Ali, M., Al-Mureikhi, M.S., Kennedy, S., Al-Thani, G., Tsui, L.C. and Teebi, A.S. (2004) A novel missense mutation in the galactosyltransferase-I (B4GALT7) gene in a family exhibiting facioskeletal anomalies and Ehlers–Danlos syndrome resembling the progeroid type. Am. J. Med. Genet. A 128A, 39–45.
[3] Quentin, E., Gladen, A., Roden, L. and Kresse, H. (1990) A genetic defect in the biosynthesis of dermatan sulfate proteoglycan: galactosyltransferase I deficiency in fibroblasts from a patient with a progeroid syndrome. Proc. Natl. Acad. Sci. USA 87, 1342–1346.
[4] Okajima, T., Fukumoto, S., Furukawa, K. and Urano, T. (1999) Molecular basis for the progeroid variant of Ehlers–Danlos syndrome. Identification and characterization of two mutations in galactosyltransferase I gene. J. Biol. Chem. 274, 28841–28844.
[5] Seidler, D.G., Faiyaz-Ul-Haque, M., Hansen, U., Yip, G.W., Zaidi, S.H., Teebi, A.S., Kiesel, L. and Götte, M. (2006) Defective glycosylation of decorin and biglycan, altered collagen structure, and abnormal phenotype of the skin fibroblasts of an Ehlers–Danlos syndrome patient carrying the novel Arg270Cys substitution in galactosyltransferase I (β4GalT-7). J. Mol. Med. 84, 583–594.
[6] Götte, M., Spillmann, D., Yip, G.W., Versteeg, E., Echtermeyer, F.G., van Kuppevelt, T.H. and Kiesel, L. (2008) Changes in heparan sulfate are associated with delayed wound repair, altered cell migration, adhesion and contractility in the galactosyltransferase I (β4GalT-7) deficient form of Ehlers–Danlos syndrome. Hum. Mol. Genet. 17, 996–1009.
[7] Esko, J.D., Kimata, K. and Lindahl, U. (2009) Proteoglycans and sulfated glycosaminoglycans in: Essentials of Glycobiology (Varki, A., Cummings, R.D., Esko, J.D., Freeze, H.H., Stanley, P., Bertozzi, C.R., Hart, G.W. and Etzler, M.E., Eds.), 2nd edn, Cold Spring Harbor Laboratory Press, Cold Spring Harbor (NY) (Chapter 16).
[8] Kreuger, J., Spillmann, D., Li, J.P. and Lindahl, U. (2006) Interactions between heparan sulfate and proteins: the concept of specificity. J. Cell Biol. 174, 323–327.
[9] Prydz, K. and Dalen, K.T. (2000) Synthesis and sorting of proteoglycans. J. Cell Sci. 113 (Pt 2), 193–205.
[10] Almeida, R., Levery, S.B., Mandel, U., Kresse, H., Schwientek, T., Bennett, E.P. and Clausen, H. (1999) Cloning and expression of a proteoglycan UDP-galactose: β-xylose β1,4-galactosyltransferase I. A seventh member of the human β4-galactosyltransferase gene family. J. Biol. Chem. 274, 26165–26171.
[11] Gulberti, S., Lattard, V., Fondeur, M., Jacquinet, J.C., Mulliert, G., Netter, P., Magdalou, J., Ouzzine, M. and Fournel-Gigleux, S. (2005) Phosphorylation and sulfation of oligosaccharide substrates critically influence the activity of human β1,4-galactosyltransferase 7 (GalT-I) and β1,3-glucuronosyltransferase I (GlcAT-I) involved in the biosynthesis of the glycosaminoglycan-protein linkage region of proteoglycans. J. Biol. Chem. 280, 1417–1425.
[12] Esko, J.D., Weinke, J.L., Taylor, W.H., Ekborg, G., Roden, L., Anantharamaiah, G. and Gawish, A. (1987) Inhibition of chondroitin and heparan sulfate biosynthesis in Chinese hamster ovary cell mutants defective in galactosyltransferase I. J. Biol. Chem. 262, 12189–12195.
[13] Bradford, M.M. (1976) A rapid and sensitive method for the quantitation of microgram quantities of protein utilizing the principle of protein-dye binding. Anal. Biochem. 72, 248–254.
[14] Bansal, S.K. and Gessner, T. (1980) A unified method for the assay of uridine diphosphoglucuronyltransferase activities toward various aglycones using uridine diphospho[U-^{14}C]glucuronic acid. Anal. Biochem. 109, 321–329.
[15] Li, D., Fournel-Gigleux, S., Barre, L., Mulliert, G., Netter, P., Magdalou, J. and Ouzzine, M. (2007) Identification of aspartic acid and histidine residues mediating the reaction mechanism and the substrate specificity of the human UDP-glucuronosyltransferases 1A. J. Biol. Chem. 282, 36514–36524.
[16] Segel, I.H. (1975) Rapid equilibrium bireactant and terreactant systemsEnzyme Kinetics, pp. 273–345, John Wiley & Sons, New York.
[17] Boeggeman, E. and Qasba, P.K. (2002) Studies on the metal binding sites in the catalytic domain of β1,4-galactosyltransferase. Glycobiology 12, 395–407.
[18] Bui, C., Ouzzine, M., Talhaoui, I., Sharp, S., Prydz, K., Coughtrie, M.W. and Fournel-Gigleux, S. (2010) Epigenetics: methylation-associated repression of heparan sulfate 3-O-sulfotransferase gene expression contributes to the invasive phenotype of H-EMC-SS chondrosarcoma cells. FASEB J. 24, 436–450.
[19] David, G., Bai, X.M., Van der Schueren, B., Cassiman, J.J. and Van den Berghe, H. (1992) Developmental changes in heparan sulfate expression: in situ detection with mAbs. J. Cell Biol. 119, 961–975.
[20] Sali, A. and Blundell, T.L. (1993) Comparative protein modelling by satisfaction of spatial restraints. J. Mol. Biol. 234, 779–815.
[21] Ramakrishnan, B., Balaji, P.V. and Qasba, P.K. (2002) Crystal structure of β1,4-galactosyltransferase complex with UDP-Gal reveals an oligosaccharide acceptor binding site. J. Mol. Biol. 318, 491–502.
[22] Case, D.A. et al. (2004) AMBER 8, University of California, San Francisco.
[23] Frisch, M.J. et al. (1998) Gaussian 98 (Revision A.11.2), Gaussian, Inc., Pittsburgh, PA.
[24] Holm, L. and Rosenstrom, P. (2010) Dali server: conservation mapping in 3D. Nucleic Acids Res. 38 (Suppl.), W545–W549.
[25] Pasek, M., Boeggeman, E., Ramakrishnan, B. and Qasba, P.K. (2010) Galectin-1 as a fusion partner for the production of soluble and folded human β-1,4-galactosyltransferase-T7 in *E. coli*. Biochem. Biophys. Res. Commun. 394, 679–684.
[26] Ramakrishnan, B. and Qasba, P.K. (2010) Crystal structure of the catalytic domain of Drosophila β1,4-Galactosyltransferase-7. J. Biol. Chem. 285, 15619–15626.